J Mater Sci (2009) 44:4047–4055
DOI 10.1007/s10853-009-3584-7

Preparation and characterization of EP/SiO_2 hybrid materials containing PEG flexible chain

Shao-rong Lu · Yu-mei Jiang · Chun Wei

Received: 25 January 2009 / Accepted: 12 May 2009 / Published online: 2 June 2009

Abstract EP/SiO_2 hybrid materials, which contained flexible chain, were prepared by epoxy resin (EP) and polyethylene glycol (PEG)-grafted polysilicic acid (PSA), which was obtained by endcapping polyethylene glycol-1000 with toluene 2,4-diisocyanate (TDI), followed by a reaction with polysilicic acid. The formation of hybrid materials was confirmed by a wide-angle X-ray diffraction (WAXD) and atomic force microscopy (AFM) analysis. Results showed that the EP/SiO_2 hybrid particles were nanosized and the average size was about 20–50 nm. The mechanical properties, dynamic mechanical properties, and thermal properties were evaluated and compared with the corresponding matrix. The improvement in impact properties in hybrid materials was explained in terms of the impact fracture surface analysis by scanning electron microscope (SEM).

Introduction

Epoxy resins (EP) have been widely used for engineering components, adhesives, electric and electronic industries and, matrix for fiber-reinforced composites owing to the exceptional combination of properties such as toughness, adhesion, and chemical resistance [1–3]. However, it is well known that the commonly used epoxy resin is generally rather brittle when cured with stoichiometric amount of common curing agents such as aliphatic or aromatic polyamides, dicarboxylic acids, anhydrides, borotrifluoride, and tertiary amines, because of its highly cross-linked structure. Its poor fracture toughness greatly limits the use of this resin in structure applications. Many efforts have been made to improve the properties of epoxy resins. They have been modified with carboxyl-terminated acrylonitrile-butadiene (CTBN) [4], amine-terminated butadiene acrylonitrile (ATBN) [5], 1,3-bis(maleimido)benzene (BMI) [6], functionally terminated acrylates, and poly (phenylene oxide) and alkylene oxides to improve their mechanical properties, and with silicone to improve thermal properties [7, 8]. However, these show the lower flexural strength and Young's modulus.

Recently, there have been a number of studies investigating the mechanical properties of particulate-reinforced epoxy composites. Incorporation of the rigid inorganic filler into various polymers or epoxy systems is a well-known technique for improving the physical, mechanical, and thermal properties. Some studies reported the epoxy modified with nano-Al_2O_3, nano-SiO_2, nano-$CaCO_3$, and nano-TiO_2, with improved properties [9–14]. Yao et al. [15] compared the storage modulus of SiO_2–epoxy nanocomposites at the glassy state and found a remarkable reinforcing effect of SiO_2 on the epoxy matrix. Zheng et al. [16] found that the impact strength of SiO_2–epoxy nanocomposites varied with SiO_2 weight content, and they attributed this change to the inhomogeneous dispersion of nanoparticles. Bauer et al. [10] found that oligomeric siloxane structures were present on the surface of coated nanoparticles due to surface modification, and a covalent bond could form between the surface-modified

---

S. Lu · Y. Jiang · C. Wei
Key Laboratory of Nonferrous Metal Materials and New Processing Technology of Ministry of Education, Guilin 541004, People's Republic of China

S. Lu (✉)
Department of Material and Chemical Engineering, Guilin University of Technology, Guilin 541004, People's Republic of China
e-mail: gllushaorong@glite.edu.cn; lushaor@163.com

nanoparticles and the epoxy resin, thus improving the thermal stability by shifting the glass transition temperature. Zhang et al. [17] reports on epoxy nanocomposites containing various contents of nanosilica particles (0–14 vol.%) prepared in situ by a special sol–gel process. The results confirmed that the homogeneously distributed nanoparticles are able to improve both the stiffness and the toughness of the epoxy.

In recent years, increasing attention has been paid to the chemical modification of the surface of silica-gel with certain functional groups, because it can improve evidently the physical and chemical properties of silica-gel. Rongjun Qu and his coworkers [18] reported the synthesis and FTIR characterization of silica-gels modified by a series of ester- and amino-terminated dendrimer-like polyamidoamine (PAMAM) grafting onto the surface of silica-gel, which exhibited good adsorption capability for Au^{3+} and Pd^{2+}. In our previously study, we have described the PEO-grafted silica sols in the epoxy/DDS curing system and found that nanoparticles could enhance tensile strength and impact strength of epoxy resin matrix [19].

In this study, polysilicic acid (PSA) surface-grafted flexible chain was obtained by endcapping PEG-1000 with toluene 2,4-diisocyanate (TDI), followed by a reaction with PSA-sol. Dynamic mechanical analysis (DMA), mechanical testing, X-ray diffraction (XRD), and scanning electron microscopy (SEM) were used to characterize the thermal, mechanical, and morphological behaviors of the hybrid materials.

Experimental

Materials

The epoxy resin used in this study is diglycidyl ether of bisphenol A (DGEBA, E-51, epoxy value = 0.51, supplied by Yueyang Chemical Plant, China, without further purification). Methyl-tetrahydrophalic anhydride methpa (MeTHPA) was purchased from Zibo kaiyu fine chemicals Limited company. *N,N*-dimethylbenzylamine was purchased from Shanghai Chemical Reagent Company, China. Polyethylene glycol (PEG-1000) was of analytical grade and was carefully got rid of water before use. Tetrahydrofuran (THF) and Sodium metasilicate ($Na_2SiO_3{\cdot}9H_2O$) were obtained from Xilong Chemical Co.Ltd. Guangdong, China. Toluene-2,4-diisocyanate (TDI) was purchased from Shanghai Chemical Reagent Company, China.

Synthesis and extraction of polysilicic acid (PSA)

The PSA was prepared according to the procedure previously used in our laboratories [20]. Typically, 19.89 g (70 mmol) of sodium metasilicate was dissolved in 70 mL water. The solution was added dropwise to 67 mL of 2.5 M HCl at 0 °C with stirring for 2 h. Silicic acid was extracted into THF by addition of 30 g of sodium chloride and 100 mL of THF. The two-phase mixture was stirred vigorously for 2 h. The aqueous layer was removed and THF solution was dried over 20 g of an hydrous sulfate to give an approximately 0.5 M silicic acid/THF solution (3.5 g of silicic acid, 89.1% SiO_2).The size and molecular weight of the nanoscaled PSA-THF solution have been determined in our previous study [20]. Its chemical structure is shown in Scheme 1.

Preparation of the flexible-chain-grafted PSA

In a 100-mL three-necked round-bottom flask, 4 g PEG-1000 dissolved in proper amount of acetone was charged with the protection of N_2 flow and heated under magnetic stirring. Once the reaction temperature reached 60 °C, the TDI acetone solution (0.6 mL of TDI dissolved in 15 mL of acetone) was added slowly drop by drop. The mixture was stirred for additional 12 h at 50–60 °C, and an orange solution was obtained. Then proper amount of PSA was dropped into the above solution and stirred at 60 °C for additional 12 h. The precursor was prepared by getting rid of acetone under vacuum at 80 °C.

Curing procedures of the EP/SiO_2 hybrid materials

In a 250-mL round-bottom flask, an appropriate amount of the flexible-chain-grafted PSA, E-51, and MeTHPA (75 g per 100 g of epoxy resin) were introduced. After vigorous stirring for 30 min, the mixture became homogenous. The

Scheme 1 Synthesis and extraction of polysilicic acid

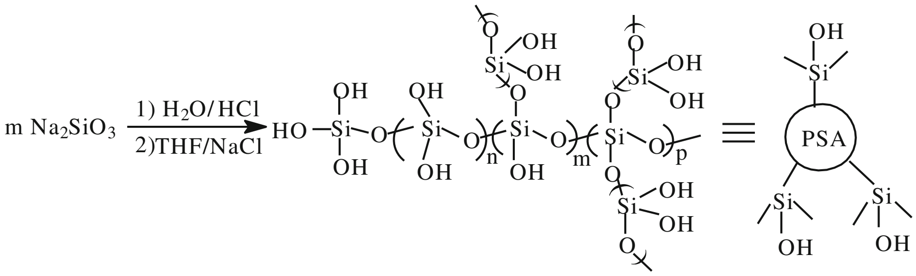

mixture was degassed in vacuum at 130 °C for about 30 min. Then *N,N*-dimethylbenzylamine was added as curing accelerator. The resulting mixture was then cast into a preheat mold coated with silicone resin. All samples were cured at 100 °C for 2 h, 130 °C for 2 h, and 150 °C for 6 h. In the curing systems, some of the interfacial force between the PEG-grafted PSA and epoxy resin had changed from the hydrogen bonding to Si–O–C covalent bond through dehydration of the hydroxyl group in epoxy resin with the residual silanol group in the PEG-grafted PSA at high temperature [21].

Measurements and instruments

Fourier transformed infrared spectroscopy (FT-IR) was recorded on a Perkin–Elmer 1710 instrument using KBr pellets at room temperature.

The impact strength was measured on a tester of type JC-25,which is with no notch in the specimen according to China National Standard GB1043-79.

The flexural strength was tested according to China National Standard GB1043-79, which is with no notch in the specimen.

The flexural strength was examined on an electron omnipotence tester of type AG-I (Shimazu, Japan). Testing machine according to China National Standard GB1040-92. The measurements of all mechanical properties in the test were made on five specimens and the average value was calculated.

Thermogravimetric analyses (TGA) was performed on powdered polymer samples with masses between 4 and 6 mg using NETZSCH STA449 from 50 to 700 °C at a heating rate of 10 °C/min under nitrogen.

Differential Scanning Calorimetry (DSC) was carried out using NETZSCH DSC 204. All tests were performed in a nitrogen atmosphere with a sample weight of about 4 mg. All samples were first heated to 200 °C at 10 °C/min and kept for 3 min to eliminate prior thermal history. The specimen was subsequently cooled down to 20 °C at a cooling rate of 10 °C/min and then heated to 200 °C at 10 °C/min.

The crystal structures of the epoxy and epoxy/SiO_2 hybrid materials were analyzed by X-ray diffractometry (XRD: D/max-RB, Japan).

The morphology of the fracture surfaces was observed by a scanning electron microscope (SEM: JSM-6380LV, Japan) at an accelerating voltage of 20 KV, and the surface was coated with a thin layer of carbon powder to reduce charge builtup on the surface and improve conductivity.

DMA was performed with a TA Instruments (Q800 dynamic mechanical analyzer) using 1 Hz frequency. The measurements were taken in the interval 40–200 °C at a heating rate of 3 °C/min.

Atomic force microscopy (AFM) was undertaken using AJ-IIIa (Shanghai AJ Nano-Science Development Co. Ltd). The scans were performed in tapping mode using silicon probes, and both height and phase images were recorded.

Results and discussion

FI-IR analysis

As mentioned in Scheme 2, synthesis of flexible-chain-grafted polysilicic acid included two steps. The first step was a hydrogen shift reaction between tolylene 2,4-diisocyanate (TDI) and PEG-1000, resulting in terminated PEG-1000. Since the molar ratio of TDI/PEG was 2/1, basically contrapuntal –NCO groups on TDI could participate in this reaction and all of the –OH groups on PEG-1000 were endcapped, with the neighboring groups remaining unreacted. In the second step the adjacent –NCO groups reacted with the –OH groups on the surface of PSA.

Figure 1 is the FT-IR spectra of (a) PSA, (b) PEG-1000, (c) endcapped PEG-1000 with TDI, and (d) PEG-grafted PSA. In (a), the peak appearing at $\sim 1075\ \mathrm{cm}^{-1}$ was assigned to Si–O–Si asymmetric stretching modes, and the wide absorptions at $3401\ \mathrm{cm}^{-1}$ were due to silanol groups (Si–OH) of PSA [22]. In (b), a distinct absorption peak at $\sim 1100\ \mathrm{cm}^{-1}$ was due to the –C–O–C stretching for ether groups and the peak at $3486\ \mathrm{cm}^{-1}$ was due to –OH group. In (c), the peak at $\sim 2274\ \mathrm{cm}^{-1}$ confirms the existence of –NCO groups. In (d), while the peak at $\sim 2274\ \mathrm{cm}^{-1}$ disappeared, the peak at $\sim 1100\ \mathrm{cm}^{-1}$ increased since the –C–O–C stretching overlapped with Si–O–C stretching band. Absorption peak at $1723\ \mathrm{cm}^{-1}$ in both (c) and (d) were mainly due to –C=O stretching vibration. The peaks at $3520\ \mathrm{cm}^{-1}$ and $3280\ \mathrm{cm}^{-1}$ were characteristic of –OH and N–H stretching, respectively. It was found that PEG-1000 was successfully grafted onto PSA through FI-IR analysis.

Figure 2 is the FT-IR spectra of (a) the neat epoxy resin and (b) the cured EP/SiO_2 hybrid materials. The absorption peak at $\sim 912\ \mathrm{cm}^{-1}$ in (b) disappeared after the curing reaction, and the results show that epoxy resin has cured completely. From1000 to $1200\ \mathrm{cm}^{-1}$ in (b), the peak broadened due to overlap with C–O–C, Si–O–C, and Si–O–Si [23].

Mechanical properties of the epoxy/SiO_2 hybrid materials

The effect of the content of silica on the toughness of epoxy/SiO_2 hybrid materials is described in Table 1. We noticed that with the flexible-chain-grafted PSA, the

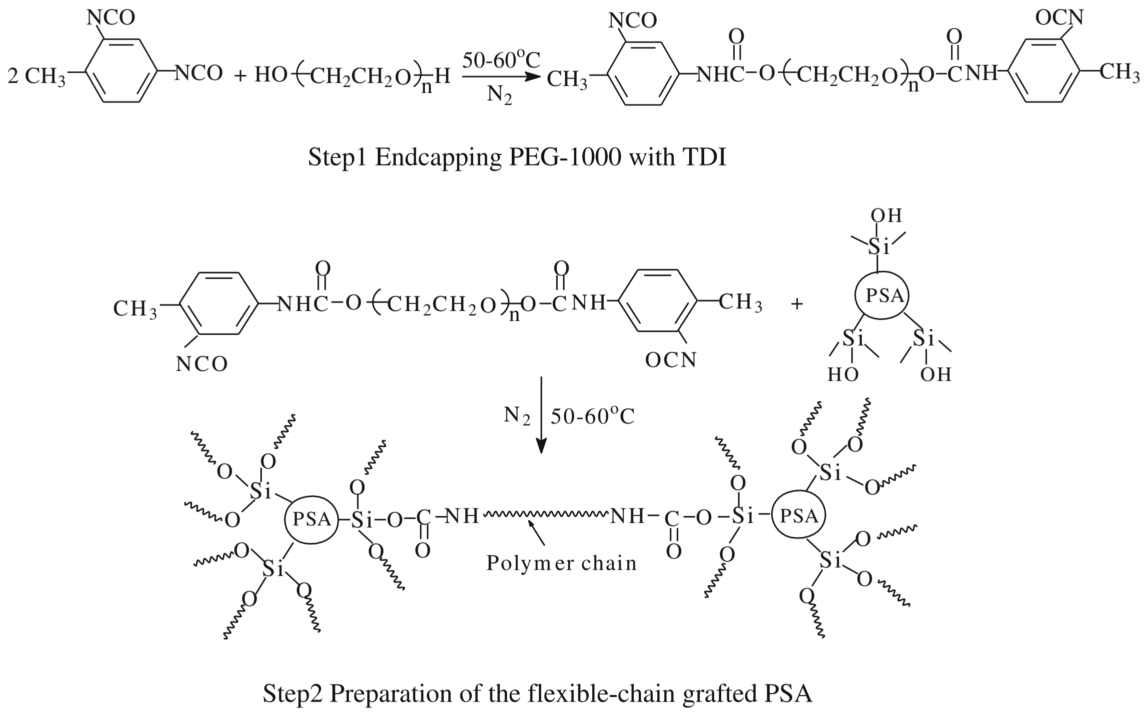

Step1 Endcapping PEG-1000 with TDI

Step2 Preparation of the flexible-chain grafted PSA

Scheme 2 Synthesis of flexible-chain-grafted Polysilicic acid

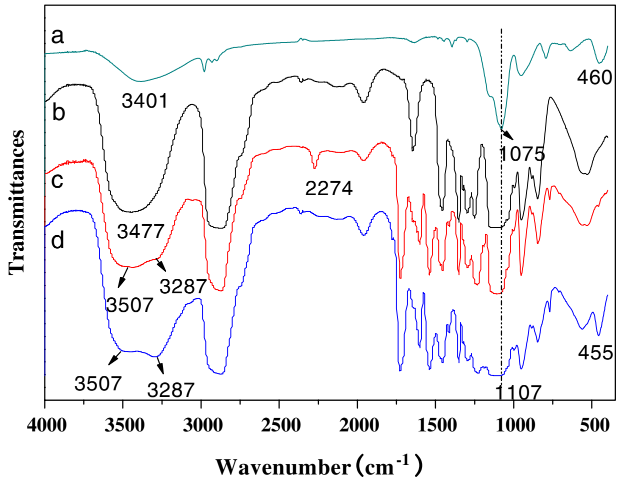

Fig. 1 Spectra of (a) PSA; (b) PEG-1000; (c) endcapped PEG-1000; and (d) PEG-grafted PSA

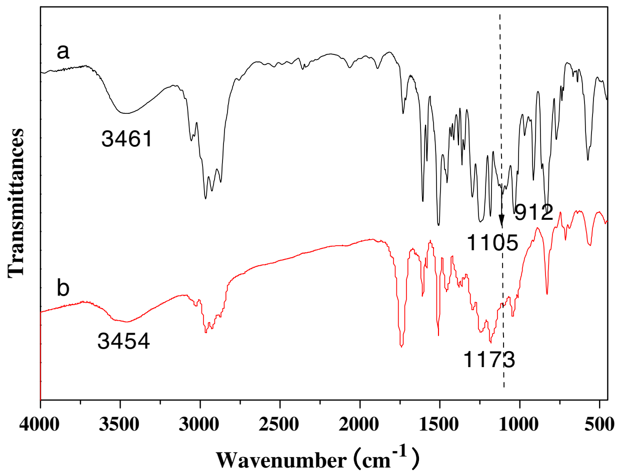

Fig. 2 Spectra of (a) the neat epoxy and (b) epoxy/silica hybrid material

toughness of epoxy/SiO_2 hybrid materials was higher than that of neat epoxy, and the impact toughness of the hybrid materials increased with increasing silica content. Since unnotched charpy impact strength reflects the energy consumed before fracture, nano-SiO_2 particles in the hybrid materials are able to induce plastic deformation of the surrounding matrix polymer to a certain extent under the condition of high strain rate. The results of Table 1 show that the impact strength reaches the highest level when SiO_2 content is about 2.0 wt%, and increases from 16.34 kJ/m^2 for the neat epoxy to 23.42 kJ/m^2; it was 43.3% higher than that of the epoxy matrix. Since nanoparticles act as strong stress concentrators, they may induce epoxy matrix yielding deformation and resistance to crack propagation [24]. Under lower SiO_2 contents, the dispersion of the particles in the epoxy matrix was good enough and the impact strength increased with the increase of the SiO_2 contents. However, the declining trend of the impact

Table 1 Mechanical properties of the epoxy/silica hybrid materials

Silica content (wt%)	Impact strength (kJ/m^2)	Tensile strength (MPa)	Tensile modulus (GPa)	Bending strength (MPa)
0	16.34	63.83	1.76	127.14
1.0	20.64	72.35	1.95	135.58
1.5	22.84	85.77	2.02	138.10
2.0	23.42	87.05	2.51	139.93
2.5	19.78	83.65	2.25	144.90
3.0	19.36	78.79	2.26	132.73

strength of the hybrid materials with increasing SiO_2 contents, it probably due to the worse distribution of the silica particles in the hybrid materials.

Table 1 shows the relation between nano-SiO_2 particles content and tensile strength and modulus. The results of the experiment indicated that the tensile strength and tensile modulus of hybrid materials increased with SiO_2 contents. When SiO_2 content is up to 2.0 wt%, the tensile strength (87.05 MPa) and modulus (2.51 GPa) of hybrid materials were higher than that of epoxy resin by 36.4% (63.83 MPa) and 42.6% (1.76 GPa), respectively. This is because when the material is subjected to a tensile test, the EP/SiO_2 hybrid materials have generated microphase separated for introducing the SiO_2 particles, which may induce epoxy matrix yielding deformation and resistance to crack propagation. Therefore, the tensile energy of the epoxy matrix is expected to decrease significantly as SiO_2 particles are introduced [25].

For the hybrid material systems containing flexible chain, flexible interface layers were formed, and there was interfacial adhesion to some extent between the dispersed phase and the matrix. Therefore, the yield strength of the hybrid materials can be higher than that of the matrix polymer. From Table 1, it is seen that flexural strength increases with increasing SiO_2. This means the interaction between PEG-grafted PSA and epoxy matrix is so strong that the nanoparticles are able to carry the applied load. The results of the experiment indicated that when the SiO_2 content is 2.50 wt%, the flexural strength (144.9 MPa) of the composite was 13.97% higher than that of epoxy resin (127.14 MPa). This increase suggests that the nanoparticles are able to introduce additional mechanisms of failure and energy consumption without blocking matrix deformation, and may induce matrix yielding under certain conditions and may furthermore act as stoppers to crack growth by pinning the cracks [24]. Nevertheless, if the fillers exceed 2.50 wt%, the failure strain undergoes a slight decay, probably due to the worse distribution of the nano-SiO_2 particles in epoxy matrix, and they reduce the matrix deformation by restraining mechanically.

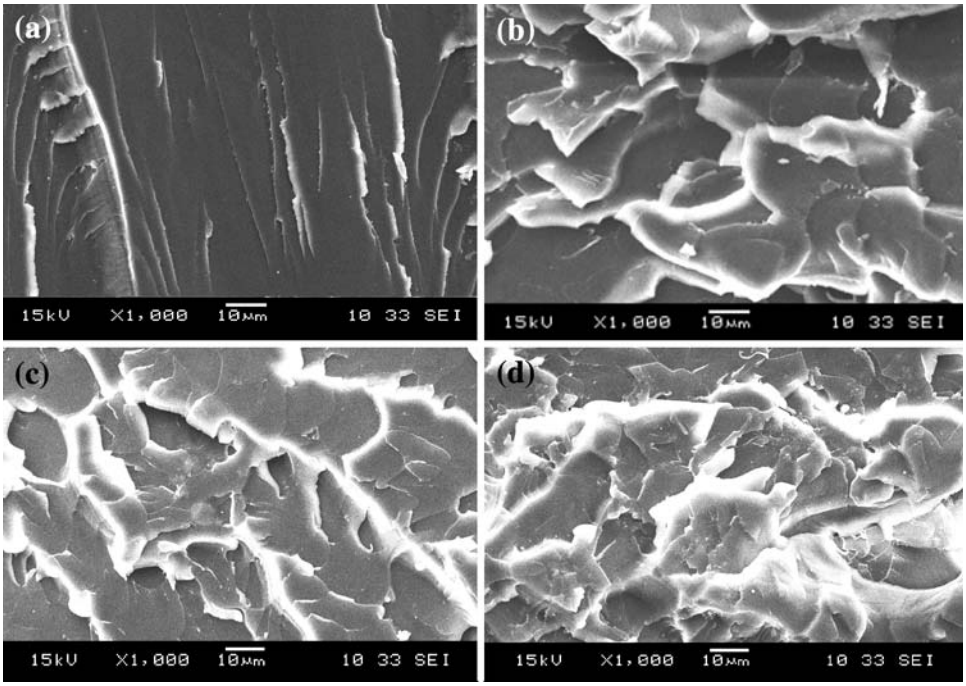

Fig. 3 SEM graphs of hybrid materials with the different SiO_2 contents **a** neat epoxy; **b** 1 wt%; **c** 2 wt%; and **d** 3 wt%

Morphological structure of hybrid materials

The fracture surfaces of neat epoxy and the hybrid materials were comparatively examined using SEM (see Fig. 3). It could be seen that neat epoxy resin exhibited a relatively smooth or glassy fracture surface with cracks almost parallel to the crack propagation direction (Fig. 3a), which is typical of a brittle thermosetting polymer [26], and shows that no large-scale plastic deformation has occurred during fracture, thus accounting for the low fracture toughness of the unfilled epoxy. These observations agree well with the low measured toughness of the materials. Compared to the case of neat epoxy, the fracture surfaces of the hybrid materials presented considerably different fractographic features (Fig. 3b–d). It can clearly be seen that the fracture stripes divert to different directions with the addition of silica-grafted flexible chain, and holes and indentations and deep cracks appeared on the fracture surfaces, indicating the characteristic of toughening facture. The increased surface roughness implied that the path of the crack tip was distorted because of the addition of nano-SiO_2 into the epoxy hybrid materials, making crack propagation more difficult. The above results unambiguously indicate that the micro-mechanism of shear yielding is the principal toughening mechanism and is responsible for the enhancement of toughness. This is in very good agreement with the impact resistance experimental data shown in Table 1.

WAXD analysis

The wide-angle (5–40°) powder X-ray diffraction (WAXD) patterns of the samples PSA, EP/silica, and reagent grade SiO_2 are shown in Fig. 4. Only a broad XRD scattering peak at 10–30° exists for the PSA and EP/silica (Fig. 4a–b), which may originate from the amorphous silica phase [27]. This result indicates that silica networks and epoxy resin chain are incorporated through the covalent bond and hydrogen bond. But reagent grade SiO_2 (Fig. 4c) showed that the peaks are very sharp, which belongs to a crystallite structure, when compared with organic polysilicic acid.

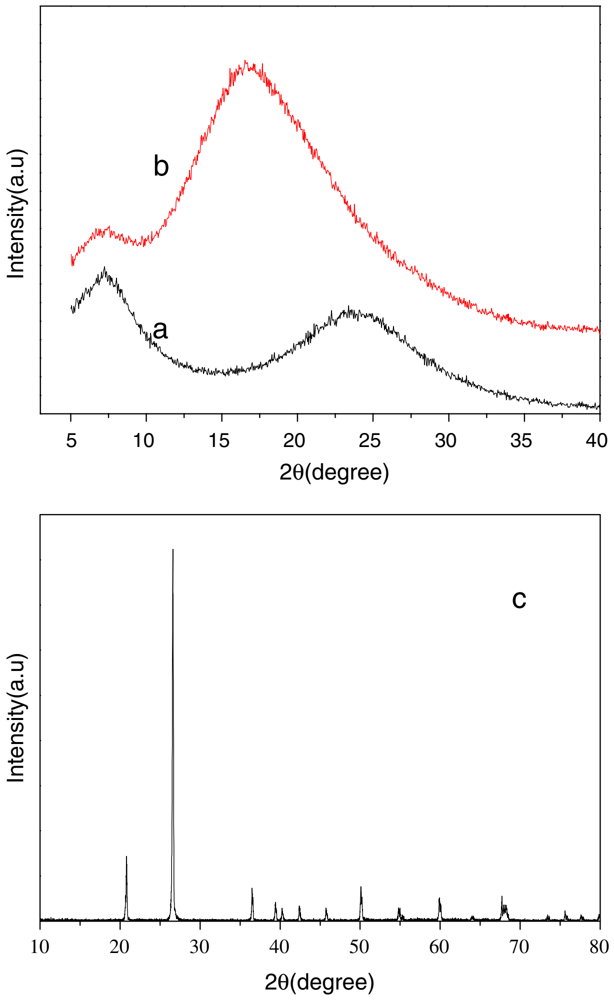

Fig. 4 Wide-angle X-ray diffraction curves of (a) PSA; (b) EP/silica; and (c) Reagent grade SiO_2

Thermal properties

Thermal gravimetric analysis (TGA) can be used not only to study the thermal decomposition and the stability of materials, but also to give important structural information. Figure 5 shows the results of the thermal decomposition of the neat epoxy resin and the hybrid materials. It is apparently seen that there was only one degradation stage on each TGA curve. When silica content is 2 wt%, the initial thermal decomposition temperature (IDT) of the EP/silica hybrid materials (371.1 °C) was increased by 10 °C compated that of the pure epoxy (361.1 °C). Nevertheless, the char yield (Y_c) of neat epoxy was nearly decomposed completely and that of hybrid materials still had retained 9.8% at 650 °C. The temperatures at the maximum weight loss rate (T_{max}) were obtained from the peak values of the TGA thermograms as shown in Fig. 6. As can be seen from the results, the thermal stability of the hybrid materials is slightly improved. The T_{max} is 14.9 °C higher than that of the neat epoxy resin when silica content is 3 wt%. The behavior is due to the presence of Si–O–Si cross-linked in the hybrid materials, which increased the polymer degradation temperature by shifting the weight-loss to higher temperature [28]. Consequently, the thermal stability of hybrid materials at high temperatures exceeds that of neat epoxy, which suggests the successful incorporation of the silica into the hybrid materials. This increase in the thermal stability can be attributed to the high thermal stability of silica and the existence of the strong interaction between the modified silica particles and the polymer matrix; a highly cross-linked density was obtained.

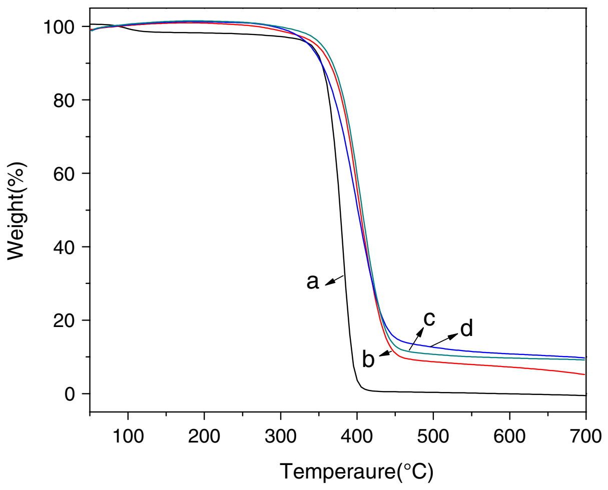

Fig. 5 TGA thermograms of (a) neat epoxy; (b) 1 wt% EP/SiO$_2$; (c) 2 wt% EP/SiO$_2$; and (d) 3 wt% EP/SiO$_2$

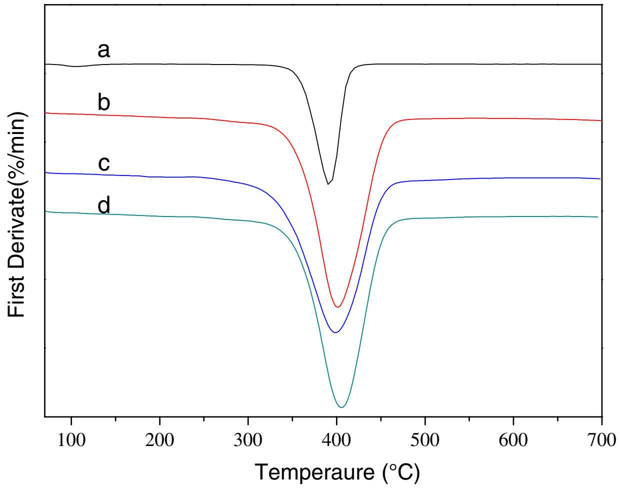

Fig. 6 Thermal decomposition rates of (a) neat epoxy; (b) 1 wt% EP/SiO$_2$; (c) 2 wt% EP/SiO$_2$; and (d) 3 wt% EP/SiO$_2$

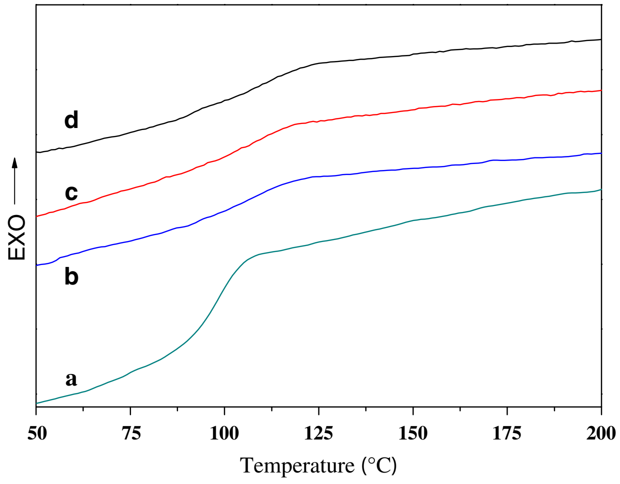

Fig. 7 DSC curves of (a) neat epoxy; (b) 1 wt% EP/SiO$_2$; (c) 2 wt% EP/SiO$_2$; and (d) 3 wt% EP/SiO$_2$

The glass transition behavior of the hybrid material is associated with cooperative motion of large chain segments, which may be hindered by the inorganic metal oxide network. The DSC traces of the EP/SiO$_2$ hybrid materials are shown in Fig. 7. It can be observed that the glass transition temperatures (T_{gs}) progressively shift to higher values with increasing SiO$_2$ content, and all data of thermal properties are listed in Table 2. The T_g of EP/SiO$_2$ samples is 123.3 °C, which is higher than that of neat epoxy resin (105.3 °C) when SiO$_2$ content is 3 wt%. The result indicates that T_g reflects an increasing interaction between the SiO$_2$ phase and the epoxy resin chain in terms of the formation of EP–Si–O– cross-links.

Dynamic mechanical behavior

Dynamic mechanical thermal analysis (DMTA) was used to determine the storage modulus (E) and the glass transition temperature (T_g) of the formulations used. Figure 8 shows that below 90 °C, the storage modulus of the EP/SiO$_2$ hybrid materials is approximate to that of the neat epoxy. But with the increasing temperature, the storage modulus in the rubbery plateau of the hybrid materials appears much higher than that of the neat epoxy. In general, dynamic modulus would decrease with the addition of the flexible chain spacer. However, PEG-grafted silica

Table 2 Data from the results of TGA and DSC

Silica content (wt%)	IDT (°C)[a]	T_g (°C)	T_{max} (°C)[b]	Y_c (%)
0	361.1	105.3	390.3	0
1	368.9	116.5	401.2	5.2
2	371.1	118.6	397.9	9.7
3	370.8	123.3	405.2	9.8

[a] The initial thermal decomposition temperature

[b] The temperatures at the maximum rate of weight loss

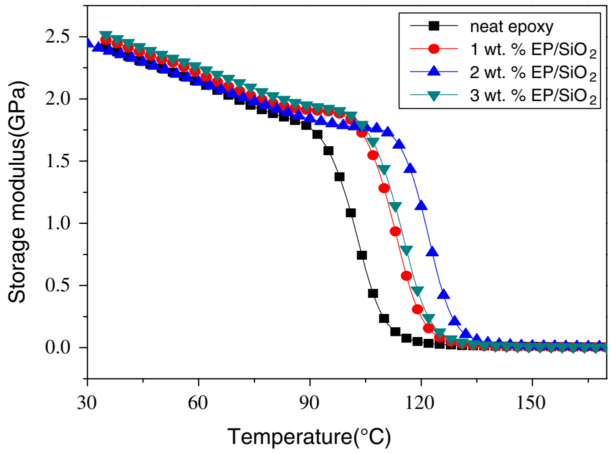

Fig. 8 Storage modulus versus temperature

particles synthesized in this study consisted of flexible chain and silica rigid particles. The flexible chain is aimed to improve impact strength, and the rigid silica particles are intended to retain high dynamic modulus and thermal properties of the EP/SiO_2 hybrid materials. The experimental results indicated that the motion of epoxy matrix chains is strongly restricted by the SiO_2 inorganic networks.

The loss tangent data of the hybrids are shown in Fig. 9. It can be seen that the tan δ peak values for the hybrid materials appear to be slightly decreased with increasing SiO_2 content. The tan δ peak temperature ($T\alpha$) for the hybrid materials is considerably higher than that of the neat epoxy. In general, $T\alpha$ of a polymer tends to increase with introduction of rigid inorganic network to epoxy matrix; in the hybrid, a covalent bond between the polymer chain and the inorganic network was formed. Kwon et al. [28] considered this to be due to the existence of interactions between particles and epoxy matrix. The addition of SiO_2 in matrix made it difficult to move the polymer chain. Therefore, the peak tanδ values decreased and glass transition temperatures (T_{gs}) were shifted to higher temperature. The reason for this may be attributed to a loss in the mobility of the chain segments of epoxy resin, resulting from the SiO_2 nano-particle/matrix interaction. The particle surface-to-surface distance should be relatively small, and the chain segment movement may be restricted.

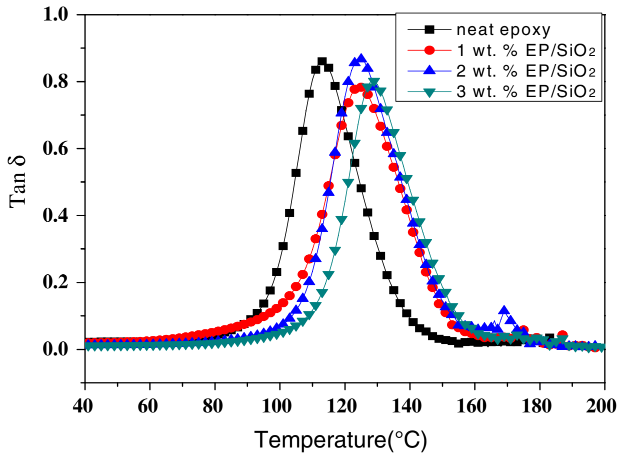

Fig. 9 Loss factor versus temperature

AFM surface image of hybrid material

The topographic morphology of epoxy/silica of hybrid material surfaces was scanned by AFM. Figure 10 reveals the representative picture (2 wt% SiO_2 content). The image shows that the organic and inorganic phases are strictly interconnected, with no major macroscopic phase separation that might occurr during the curing process. The 3D image revealed a surface roughness (R_{ms}) of 0.73 nm, and the silica particles size is about 20–50 nm in diameter. The image may demonstrate that a strong bond has been formed between the PEO-grafted PSA sols and the epoxy matrix in the hybrid material. This indicates that SiO_2 particles are homogeneous and well dispersed in the hybrid material matrix.

Conclusion

In this study, epoxy resin/SiO_2 hybrid materials were prepared by epoxy resin and PEG-grafted silica particles using MeTHPA as curing agent. The experimental results showed the silica particle size in the hybrid films was about 20–50 nm, and the nano-SiO_2 domains disperse homogeneously in epoxy matrix without macro-phase separation. The studies of the mechanical properties and the analysis of the SEM images of the epoxy/SiO_2 hybrids showed that

Fig. 10 AFM surface images of the hybrid material specimen

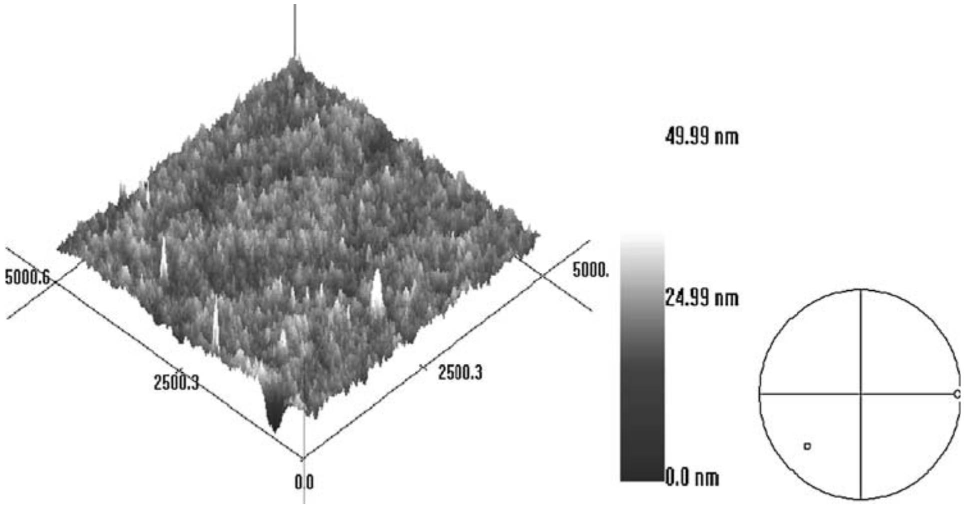

incorporation of flexible chains to silica could effectively toughen the epoxy resin because of the SiO_2 particles perturbing the crack front and thus altering the path of the propagating crack. The glass transition temperatures (T_{gs}) and the tan δ peak temperature ($T\alpha$) of EP/SiO_2 hybrid materials shift toward higher temperatures perhaps due to the presence of silica that are strongly bonded with the epoxy matrix. The thermal stability of EP/SiO_2 hybrid materials is higher than that of the neat epoxy resin at high temperature.

Acknowledgements The authors are grateful for the financial support by the National Natural Science Foundation of China (No. 50763001), the Natural Science Foundation of Guangxi Province, China (No. 0991003Z), the Scientific Research and Technology Development Plan of Guangxi Province of China (No. 0842003-4A), and the Funding Scheme Talents of Guangxi Province, China (No. 0817).

References

1. Johnsen BB, Kinloch AJ, Mohammed RD et al (2007) Polymer 48:530
2. Yee AF, Pearson RA (1986) J Mater Sci 21:2462. doi:10.1007/BF011142932462-2474
3. Kinloch AJ, Shaw SJ, Hunston DL et al (1983) Polymer 32:1341
4. Mitsukazu O, Takahide M, Shinobu K et al (2001) Polymer 42:9687
5. Chikhi N, Fellahi S, Bakar M (2002) Eur Polym J 38:251
6. Dinakaran K, Alagar M, Suresh Kumar R (2003) Eur Polym J 39:2225
7. Wu CS, Liu YL, Chiu YS (2002) Polymer 43:4277
8. Ho TH, Wang CS (2001) Eur Polym J 37:267
9. Zhai L, Ling G, Li J, Wang Y (2006) Mater Lett 60:3031
10. Bauer F, Decker U, Ernst H, Findeisen M et al (2006) J Adhes Adhes 26:567
11. Zhang X, Xu W, Xia X, Zhang Z et al (2006) Mater Lett 60:3319
12. Zunjarrao SC, Singh RP (2006) Epoxy Resins Sci Technol 66:2296
13. Yu HJ, Wang L, Shi Q, Jiang GH et al (2006) Prog Org Coat 55:296
14. Li H, Zhang Z, Ma X, Hu M et al (2007) Surf Coat Technol 201:5269
15. Yao XF, Yeh HY, Zhou D, Zhang YH (2006) J Compos Mater 40:371
16. Zheng Y, Zheng Y, Ning R (2003) Mater Lett 57:2940
17. Zhang H, Zhang Z, Friedrich K et al (2006) Acta Materialia 54:1833
18. Qu R-J, Niu Y-Z, Sun C-M et al (2006) Microporous Mesoporous Mater 97:58
19. Lu S-R, Wei C, Yu J-H et al (2006) J Mater Sci 42:6708. doi:10.1007/s10853-006-1492-7
20. Lu S-R, Zhang H-L, Zhao C-X et al (2005) J Mater Sci 40:1079. doi:10.1007/s10853-005-6920-6
21. Hsu YG, Lin KH, Chiang IL (2001) Mater Sci Eng B87:31
22. Merzbacher CI, White B (1991) J Non-Cryst Solids 18:130
23. Nishio K, Okubo K, Watanabe Y et al (2000) J Sol-Gel Sci Technol 19:187
24. Wetzel B, Haupert F, Zhang MQ (2003) Compos Sci Technol 63:2055
25. Kinloch AJ, Taylor AC (2002) J Mater Sci 37:433. doi:10.1023/A:1013735103120433-460
26. Gao F, Lu Q, Liu X, Yan Y et al (2001) Nano Lett 1:743
27. Liu P, Song J, He L et al (2008) Eur Polym J 44:940
28. Kwon S-C, Adachi T, Araki W (2008) Composites B Eng 39:773